Development and application of aerosol data assimilation in NICAM

Tie Dai[1], Yueming Cheng[1], Daisuke Goto[2], Guangyu Shi[1], and Teruyuki Nakajima[3]

1. State Key Laboratory of Numerical Modeling for Atmospheric Sciences and Geophysical Fluid Dynamics, Institute of Atmospheric Physics, Chinese Academy of Sciences, Beijing, China
2. National Institute for Environmental Studies, Tsukuba, Japan
3. Earth Observation Research Center, Japan Aerospace Exploration Agency, Tsukuba, Japan

2019.2.1

Can observations improve model to simulate the aerosol distribution and its impact?

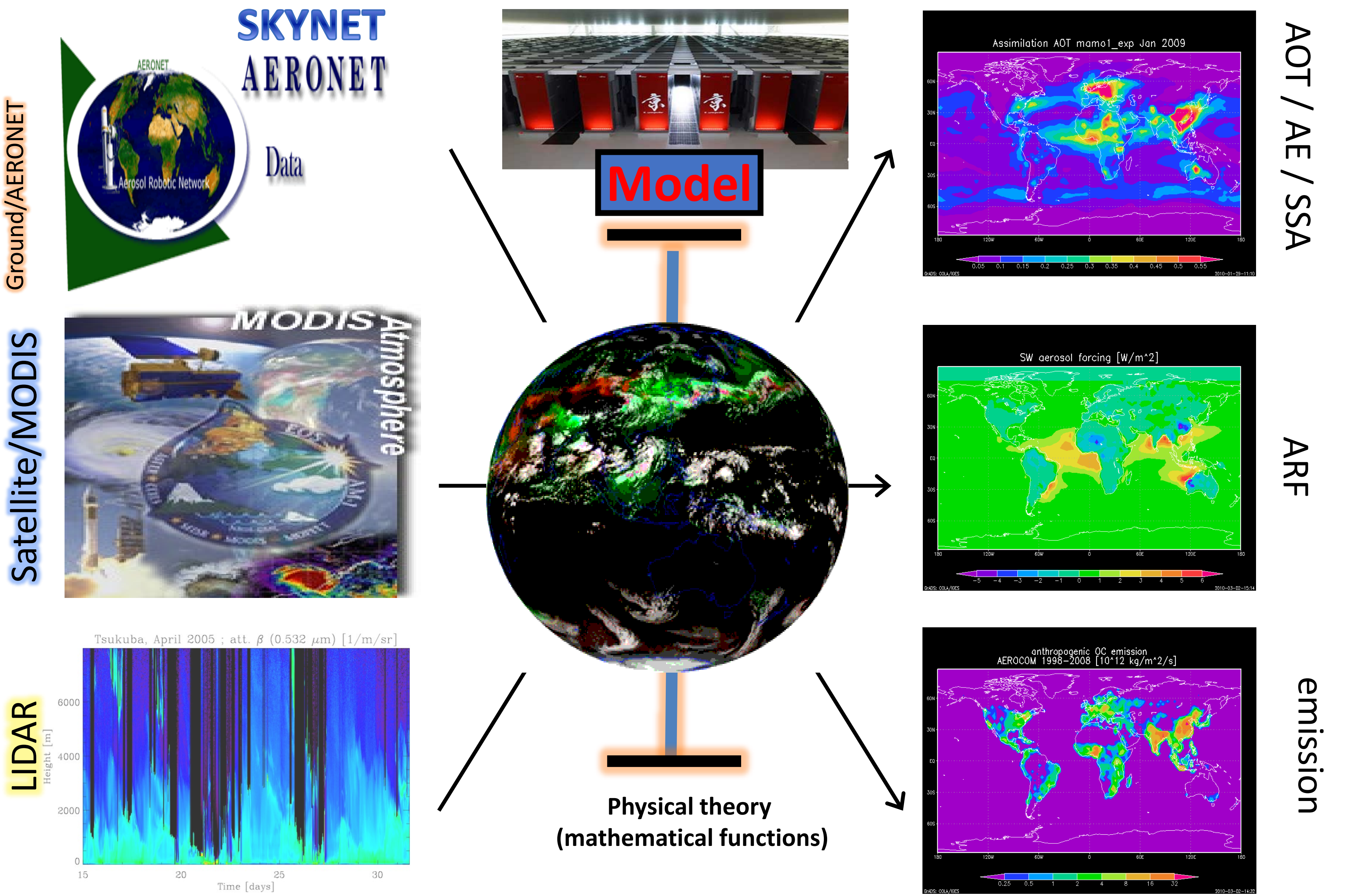

Forward Model：Global and regional high-resolution model NICAM-Chem

Science AAAS

A Madden-Julian Oscillation Event Realistically Simulated by a Global Cloud-Resolving Model
Hiroaki Miura *et al.*
Science **318**, 1763 (2007);
DOI: 10.1126/science.1148443

b

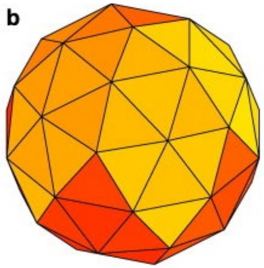

Quasi-homeg. grid

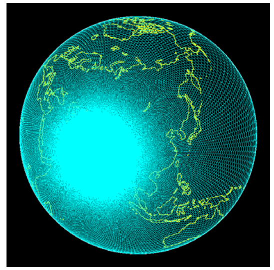

Stretched-grid

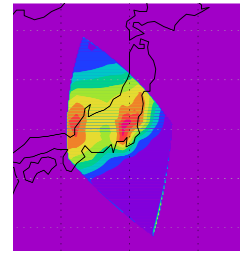

Regional-grid

Radiation: MSTRN (Sekiguchi&Nakajima, JQSRT'05)

SPRINTARS aerosols	CHASER short-lived gases (O3 etc)	TM (CO_2 etc)	Isotopes (HDO etc)
Takemura et al.(JGR'00)	Sudo et al. (JGR'02)	Niwa et al. (ACP'11)	Yoshimura et al. (JGR'14)

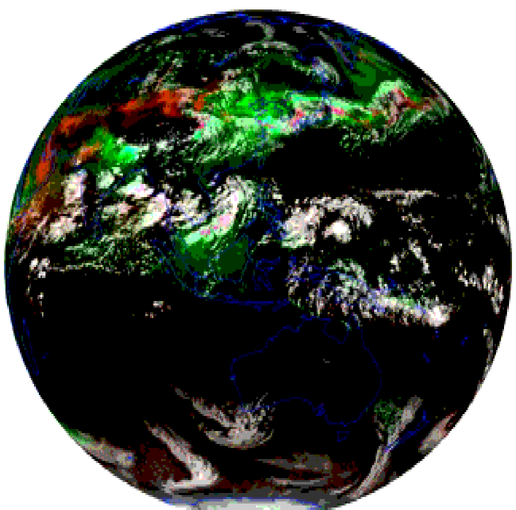

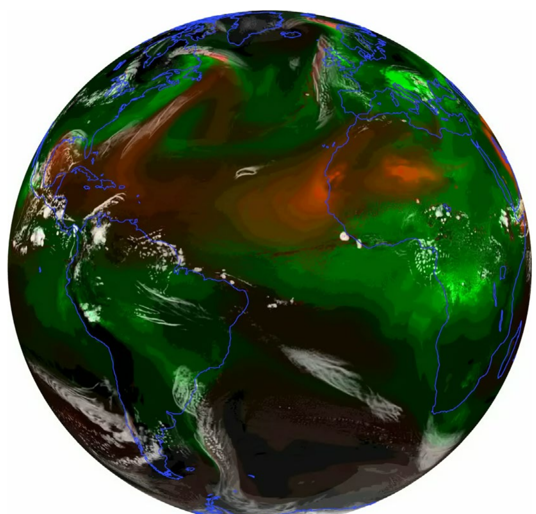

7km simulation on the Earth Simulator
cloud, mineral dust, Fine aerosols (*Suzuki et al., GRL'08*)

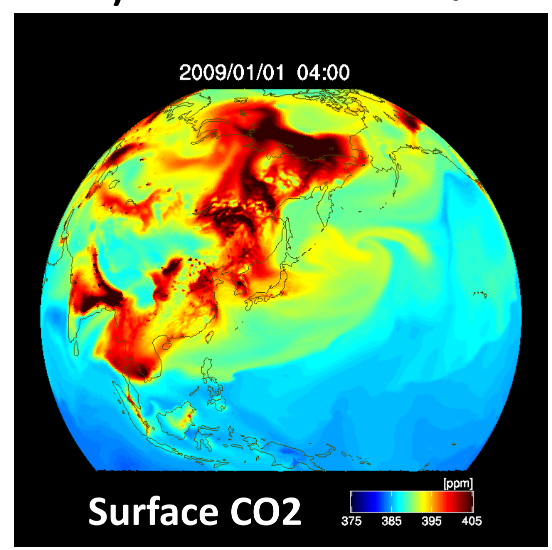

Stretched grid simulation

Global online aerosol model: NICAM+SPRINTARS

Spectral Radiation-Transport model for Aerosol
(Takemura et al., 2000, 2002, 2005, 2009)

- NCEP, NCEP-FNL or GPV-JMA

- Cloud microphysics: Large scale condensation, NSW6
- Arakawa-Schubert cumulus convection
- MATSIRO land surface model

- Sea salt: w_{10} (Ericksson or Monahan)
- Mineral dust: w_{10} , vegetation, soil moisture, snow cover, LAI
- Sulfate: fossil fuel, biomass burning, volcanoes
- Carbons (OC&BC): fossil fuel, biomass burning, agricultural activities, plant emissions
- Chemistry: sulfur oxidation, (SOA chemistry, nitrate thermal eq.)
- Removal through wet & dry deposition, gravitational settling

METEOROLOGY REANALYSIS → NICAM GCRM ↔ Meteorological & Cloud field ↔ SPRINTARS AEROSOL MODULE

P, Wind speeds, Temperature, specific humidity, Cloud

Aerosol mass mixing ratio: dust (10 bin), Sea salt (4 bin), OC, BC, Sulfate,SO2

K-distribution Radiative Transfer Model

Direct aerosol effect on radiative balance; 1st and 2nd indirect aerosol effects on clouds

Local Ensemble Transform Kalman Filter
(LETKF, Ott et al.2004, Hunt et al., 2007, Miyoshi et al 2007a,b)

$$\Psi(\mathbf{x}_a) = (\mathbf{y} - \mathbf{H}\mathbf{x}_a)^T \mathbf{R}^{-1} (\mathbf{y} - \mathbf{H}\mathbf{x}_a) + (\mathbf{x}_f - \mathbf{x}_a)^T \mathbf{P}^{-1} (\mathbf{x}_f - \mathbf{x}_a)$$

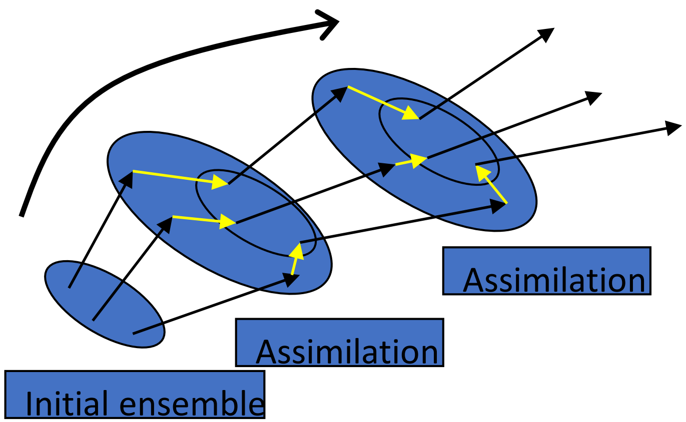

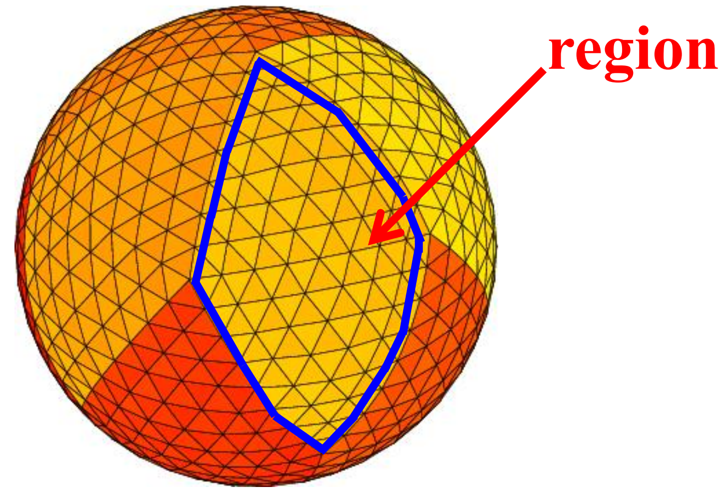

1. The assimilation system uses the some grid and regional system as the forward model (NICAM-SPRINTARS), so it is convenient to use the forward model forecast variables.
2. The observation sites are searched in each region at the same time. If one site is found, the simulated observation will be calculated and transmit it to all of the other processors to generate the global observations.
3. In every grid point, each processor assimilate the useful observation based on the distance between the observation site and the grid point.
4. Output the analysis results for the next forward calculation.

Observation operater (H): transfer the control variables (fine and coarse aerosol masses) to observed aerosol optical properties

72 *T. Dai et al. / Atmospheric En*

Table 1
Particle density, particle radius, refractive index, mass extinction coefficient (β), AE derived from β at 440 and 870 nm, and SSA for dry aerosol as used in the model.

Species	Density (g cm^{-3})	dry particle radius (μm)	Refractive index at 550 nm	β at 550 nm (m^2 g^{-1})	AE	SSA
Sulfate	1.769	0.0695	1.43−10^{-8}i	1.775	2.740	1.000
BC	1.25	0.0118	1.75−0.44i	8.185	1.119	0.323
OC	1.5	0.02	1.53−0.006i	1.062	2.683	0.915
OC/BC (1)	1.473	0.1	1.558−0.063i	5.455	1.520	0.766
OC/BC (2)	1.468	0.1	1.563−0.072i	5.547	1.478	0.741
OC/BC (3)	1.442	0.1	1.588−0.126i	6.036	1.278	0.638
OC/BC (4)	1.462	0.1	1.569−0.085i	5.666	1.426	0.712
OC/BC (5)	1.468	0.1	1.563−0.072i	5.547	1.478	0.741
Dust	2.5	0.13	1.53−0.0055i	2.239	2.811	0.965
	2.5	0.20	1.53−0.0055i	3.809	1.838	0.976
	2.5	0.33	1.53−0.0055i	3.652	0.608	0.972
	2.5	0.52	1.53−0.0055i	2.059	−0.405	0.950
	2.5	0.82	1.53−0.0055i	1.013	−0.348	0.903
	2.5	1.27	1.53−0.0055i	0.687	−0.081	0.876
	2.5	2.02	1.53−0.0055i	0.397	−0.010	0.831
	2.5	3.20	1.53−0.0055i	0.248	−0.047	0.778
	2.5	5.06	1.53−0.0055i	0.155	−0.0530	0.719
	2.5	8.02	1.53−0.0055i	0.089	−0.041	0.652
Sea salt	2.2	0.178	1.50−10^{-8}i	4.257	1.850	1.000
	2.2	0.562	1.50−10^{-8}i	1.715	−0.352	1.000
	2.2	1.78	1.50−10^{-8}i	0.493	0.011	1.000
	2.2	5.62	1.50−10^{-8}i	0.168	−0.078	1.000

Note: OC/BC (1−5) represent the internal mixture of OC and BC for tropical forest fire, other forest fire, fossil fuel, fuel wood, and agriculture source, respectively. The β and SSA for sulfate, BC, OC, OC/BC, and sea salt are calculated from the Mie-scattering theory using a mono-modally lognormal size distribution. The modal radii (r_m) for sulfate, BC, OC, OC/BC, and sea salt are 0.0695, 0.0118, 0.02, 0.1, and 0.114 μm, while the geometric standard deviations (σ_g) are 1.526, 2.3, 1.8, 1.562, and 2.305, respectively. The size distribution for dust aerosol is assumed a bi-modally lognormal distribution with $r_m = 0.202, 0.994$ μm and $\sigma_g = 2.397, 1.110$.

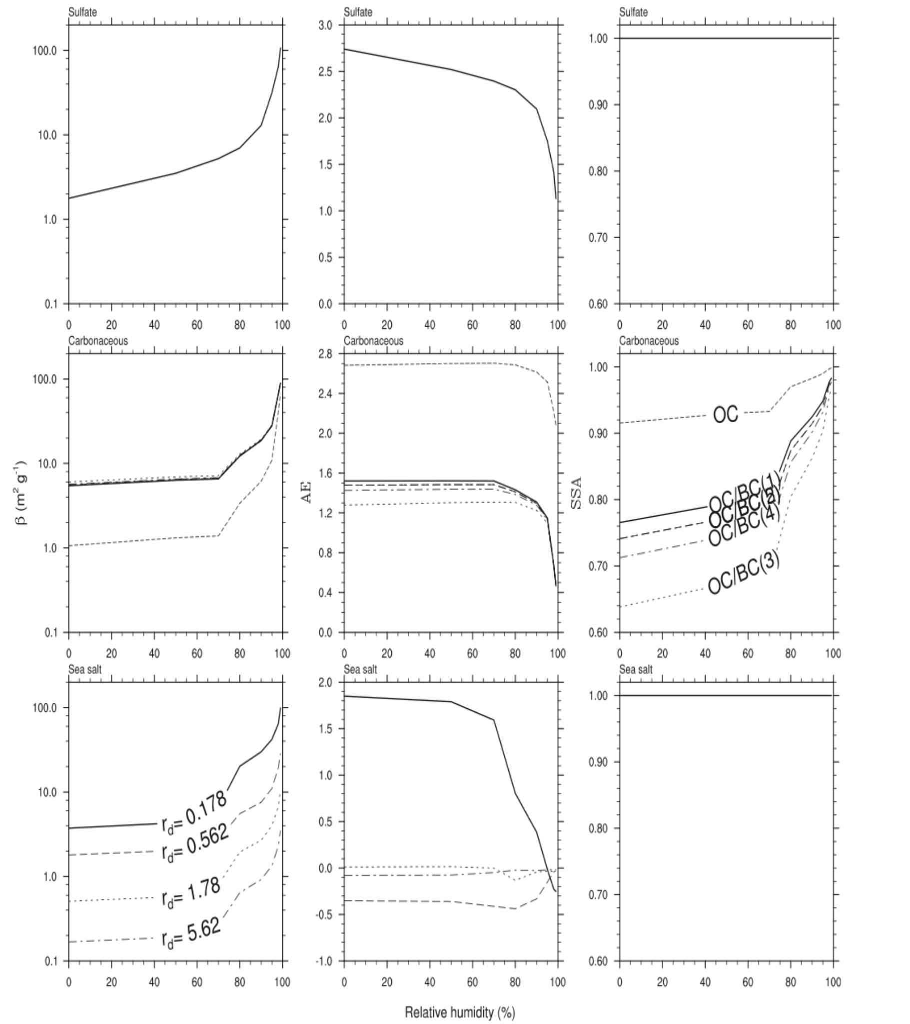

Fig. 1. Mass extinction coefficient (β) at 550 nm (left column), AE derived from β at 440 and 870 nm (middle column), and SSA at 550 nm (right column) for sulfate, carbonaceous aerosols, and sea salt as a function of relative humidity. Here, OC/BC (1–5) represent the internal mixture of OC and BC for tropical forest fire, other forest fire, fossil fuel, fuel wood, and agriculture source, respectively. Four different sizes of sea salt are shown with respective dry radius (r_d).

MODIS observations and experiment setting (LETKF with every 6 hours)

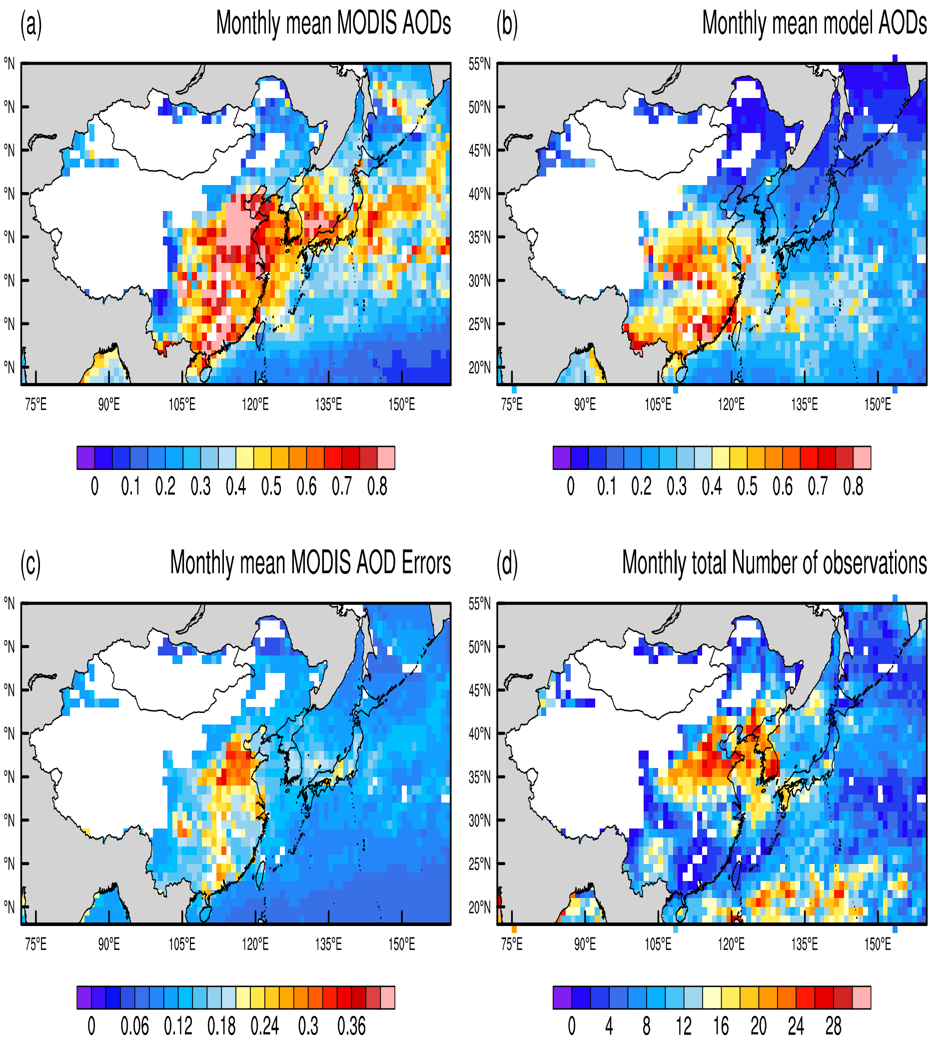

Dai et al, 2014, Environmental Pollution

Period: 2006 April

Asian Dust occurs frequently

Random perturb the standard aerosol emissions with standard deviations 1to generate the ensemble members

Table 1

Experimental design for the sensitivity test in this study.

Sensitivity experiments
Exp1: 10 ensemble members; spatiotemporally dependent perturbation factors; with a local patch radius of 1500 km
Exp2: same as Exp1 but spatiotemporally independent perturbation factors
Exp3: same as Exp1 but 20 ensemble members
Exp4: same as Exp2 but 20 ensemble members
Exp5: same as Exp1 but 40 ensemble members
Exp6: same as Exp2 but 40 ensemble members
Exp7: same as Exp1 but local patch radius of 1000 km
Exp8: same as Exp1 but local patch radius of 2000 km
Exp9: standard NICAM + SPRINTARS
Exp10: free run with 10 ensemble members and spatiotemporally dependent perturbation factors
Exp11: free run with 10 ensemble members and spatiotemporally independent perturbation factors

Sensitivity to the Kalman filter parameters

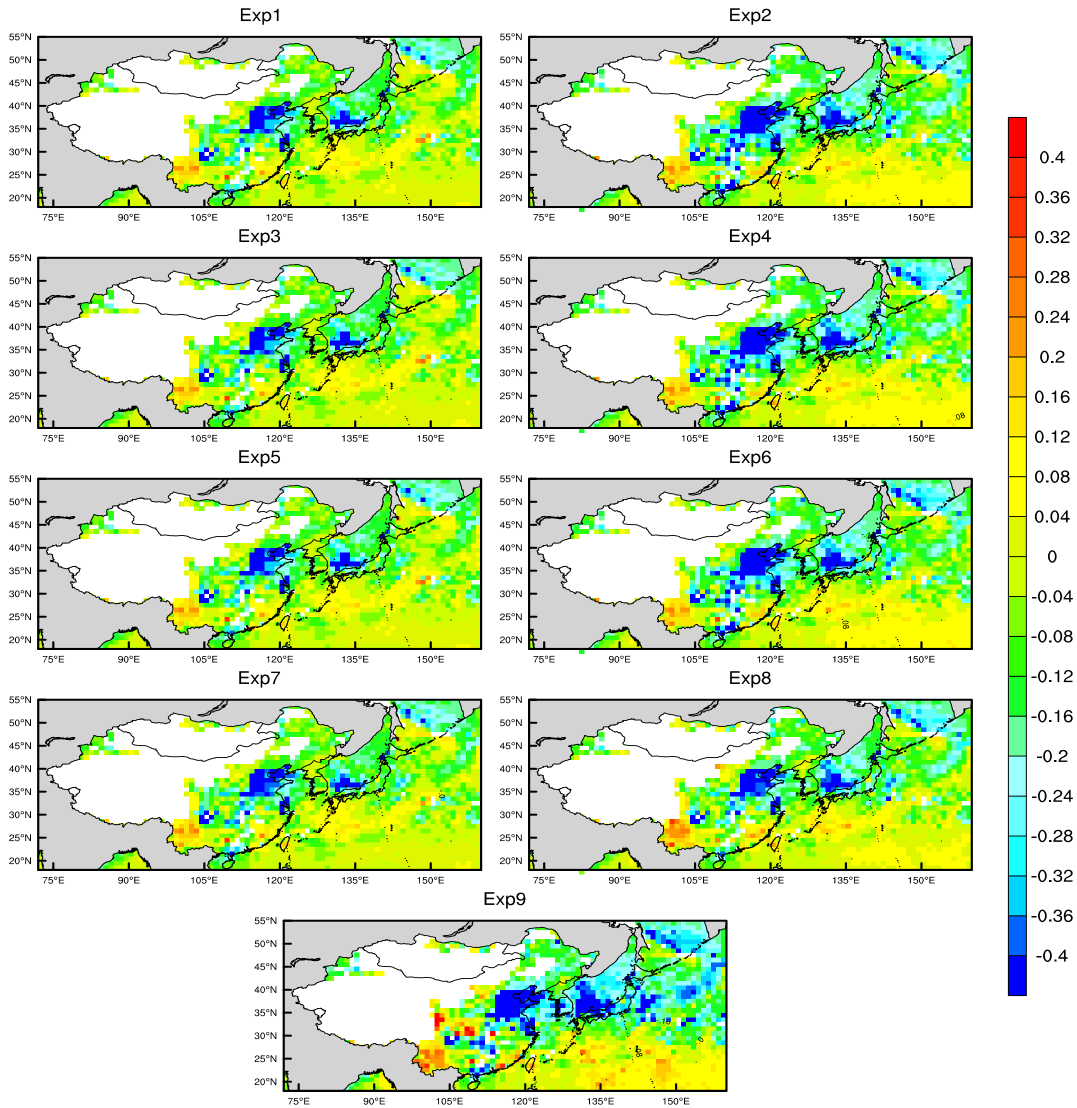

1) The perturbation method has the largest influence on the performance of the assimilation compared with the ensemble and local patch sizes.
2) The general spatiotemporally independent random perturbation factors tend to yield a low estimation of the model uncertainties and the analyses are affected by an overconfidence in the modeled estimate
3) The perfect spatiotemporally dependent modification factors looks to be a better choice.

Validation using the AERONET observations

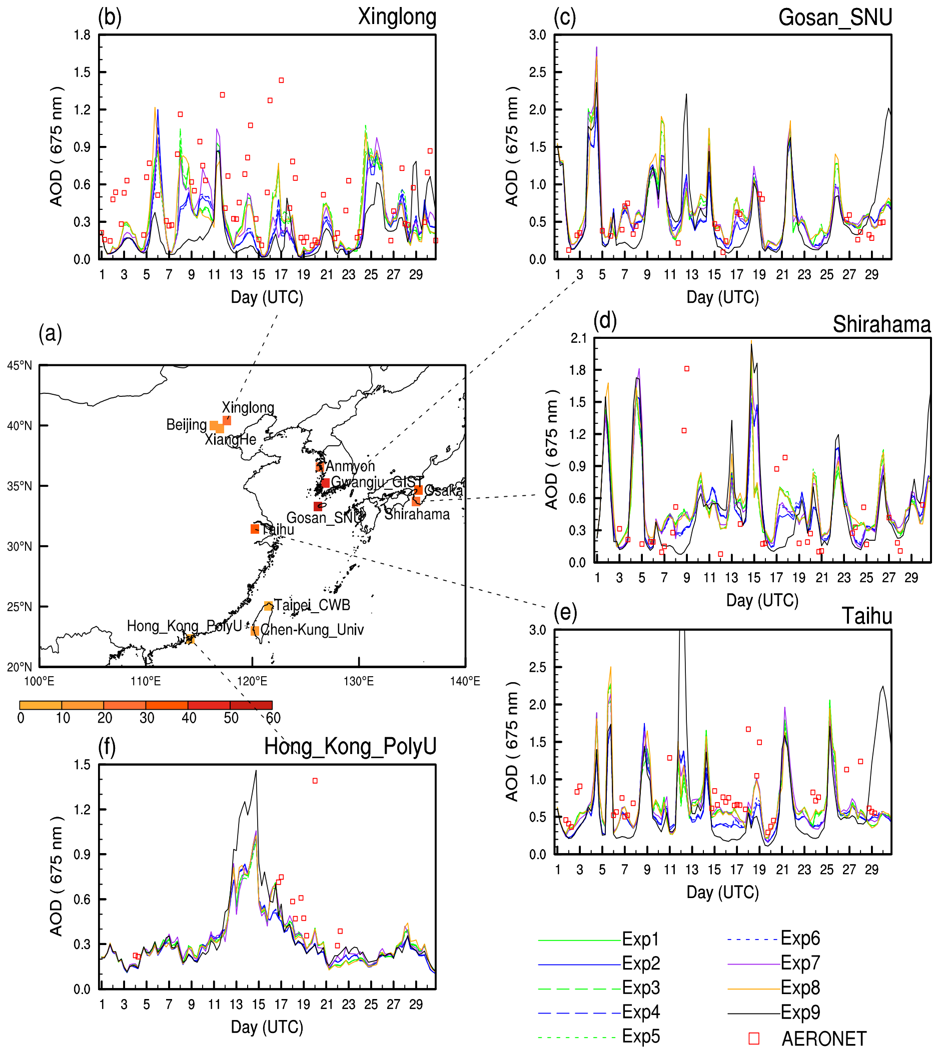

Table 2

Summary of the statistics for the modeled and AERONET observed AOD comparisons.[a]

Site name	N	M_o	B_s	B_a	R_s	R_a	AEC
Beijing	61	0.943	−0.780	−0.677 (↑)	0.162	0.411 (↑)	10.47
Xinglong	66	0.577	−0.420	−0.306 (↑)	0.300	0.720 (↑)	22.70
Xianghe	62	0.881	−0.705	−0.607 (↑)	0.116	0.528 (↑)	12.64
Anmyon	19	0.631	−0.469	−0.242 (↑)	0.188	0.463 (↑)	24.53
Gwangju_GIST	12	0.557	−0.340	−0.113 (↑)	−0.145	0.597 (↑)	49.31
Gosan_SNU	27	0.436	−0.068	0.057 (↑)	0.046	0.638 (↑)	56.62
Osaka	25	0.497	−0.228	−0.126 (↑)	0.065	0.498 (↑)	35.65
Shirahama	30	0.372	−0.097	0.011 (↑)	−0.231	0.252 (↑)	23.54
Taihu	36	0.734	−0.393	−0.249 (↑)	0.124	0.549 (↑)	35.56
Taipei_CWB	16	0.468	−0.139	−0.179 (↓)	−0.453	−0.254 (↑)	3.96
Chen-Kung_Univ	18	0.271	0.024	0.004 (↑)	0.320	0.580 (↑)	14.54
Hong_Kong_Polyu	13	0.621	−0.326	−0.308 (↑)	0.340	0.512 (↑)	5.75

[a] Note. Shown are the site name, the number of the total available model-observed pairs (***N***), monthly mean AERONET observed AOD (***M*₀**), the mean bias of the standard model (***B*ₛ**), the mean bias of the assimilation experiment Exp1 (***B*ₐ**), the correlation coefficient of the standard model (***R*ₛ**), the correlation coefficient of the assimilation experiment Exp1 (***R*ₐ**), and the assimilation efficiency of the experiment Exp1 (AEC). The symbol ↑ indicates the modeled results are improved by the assimilation, whereas the symbol ↓ indicates the modeled results are worsened by the assimilation.

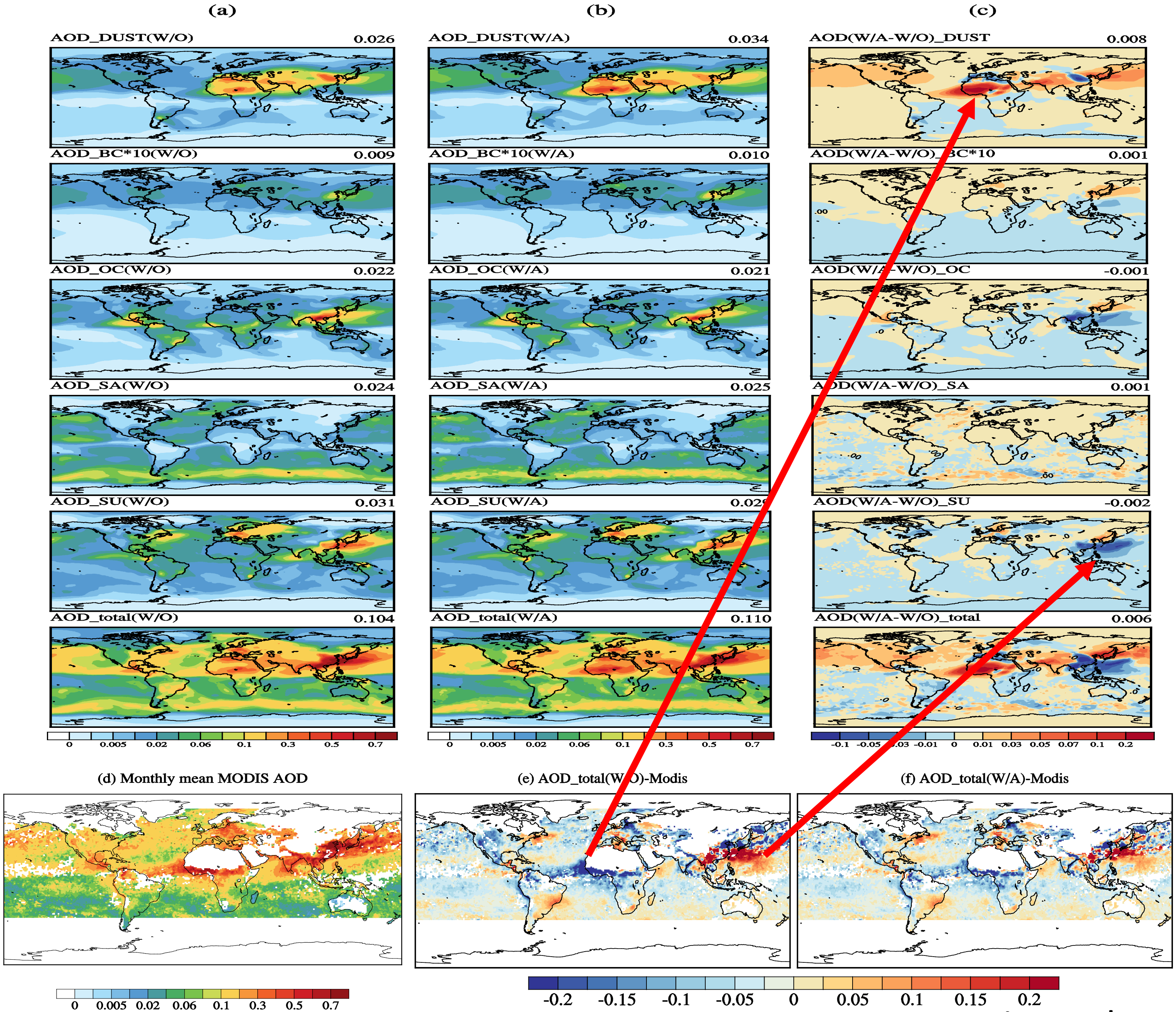

Yin et al, AR, 2016

Validation over Chinese desert regions

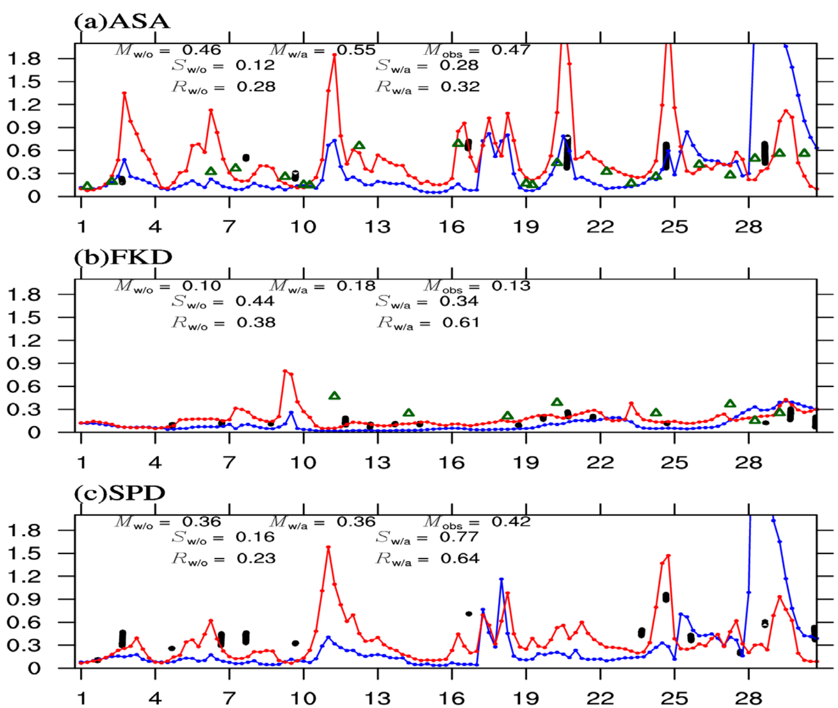

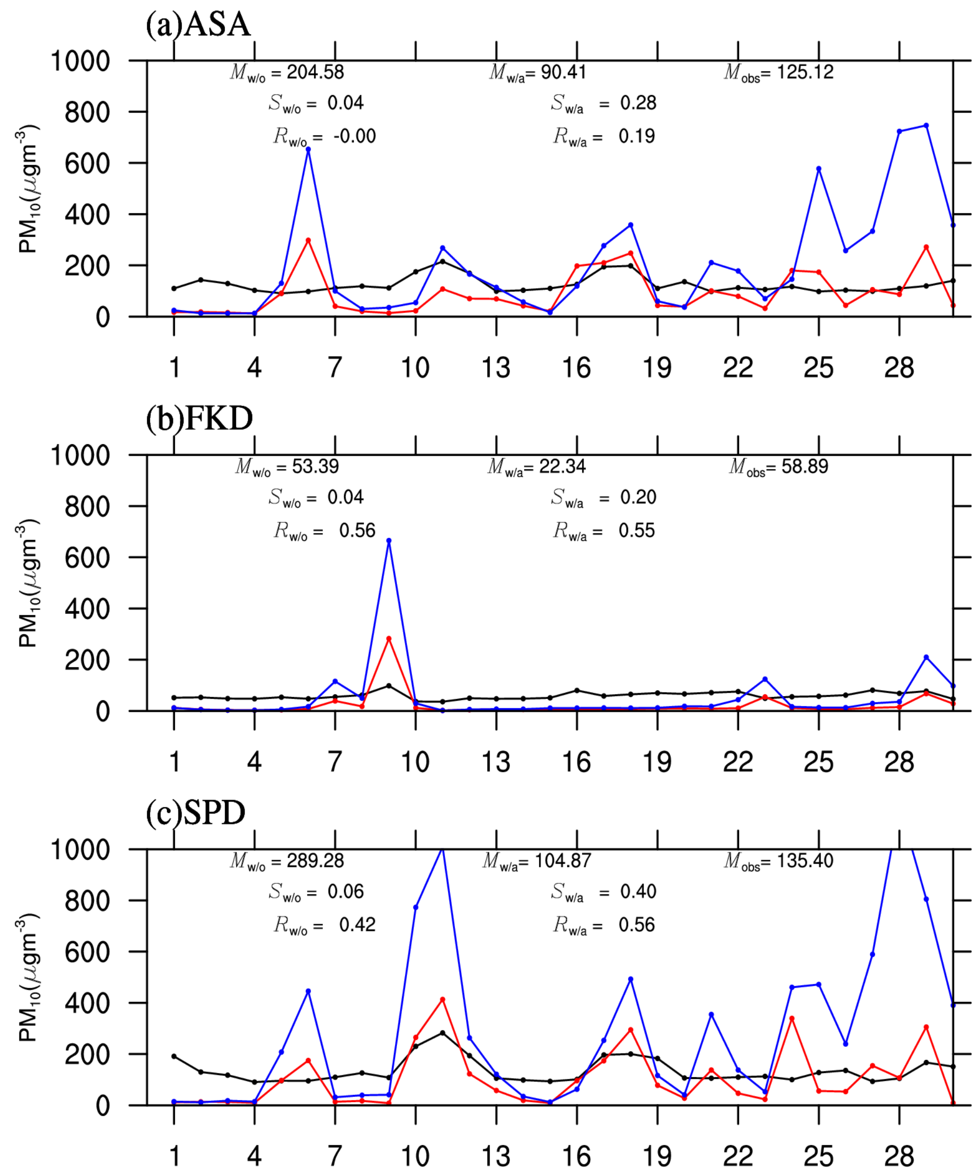

Geostationary satellites have higher observation frequency than the conventional polar orbiting satellites.

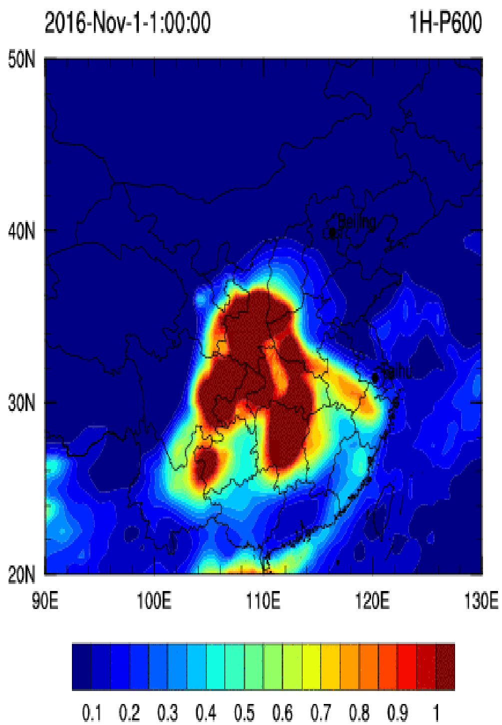

Model result

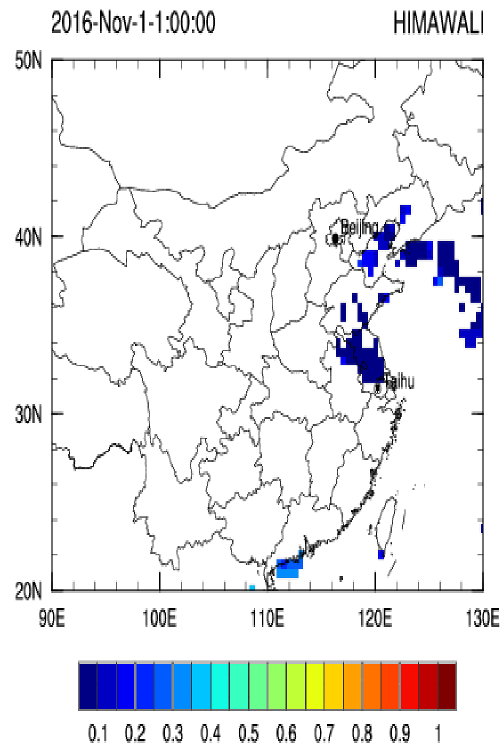

Geostationary satellite: Himawari-8

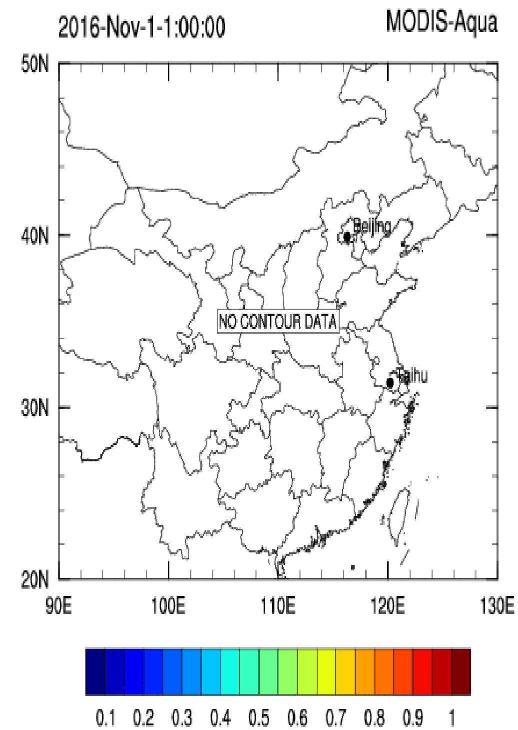

Conventional polar orbiting satellite: MODIS

The comparison between Himawari-8, MODIS and AERONET

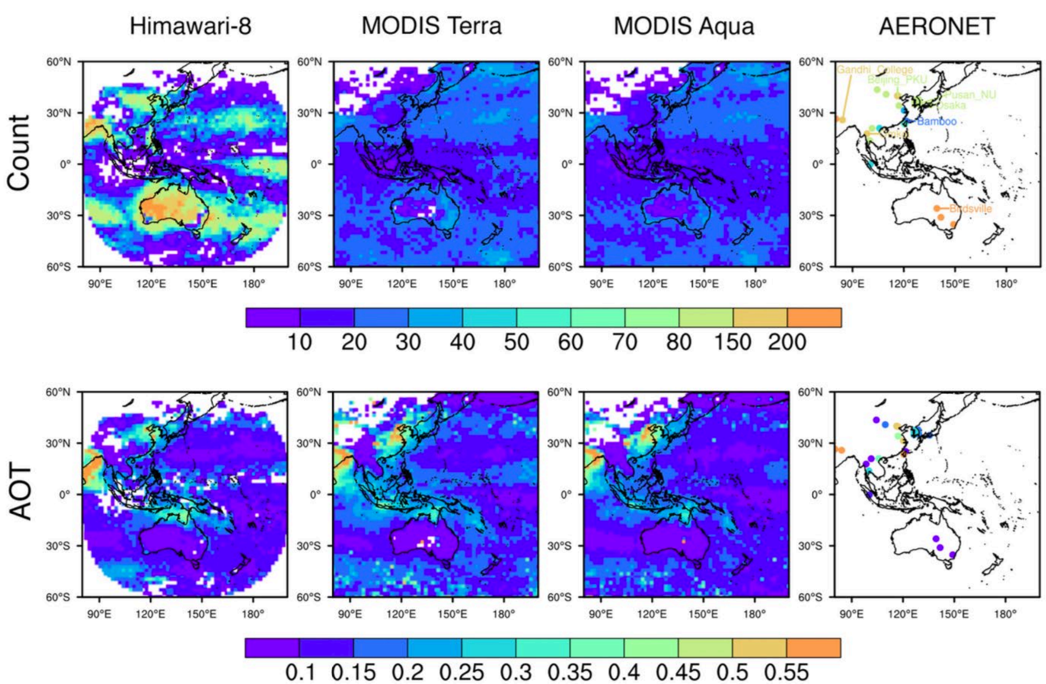

The differences of Himawari-8 minus MODIS

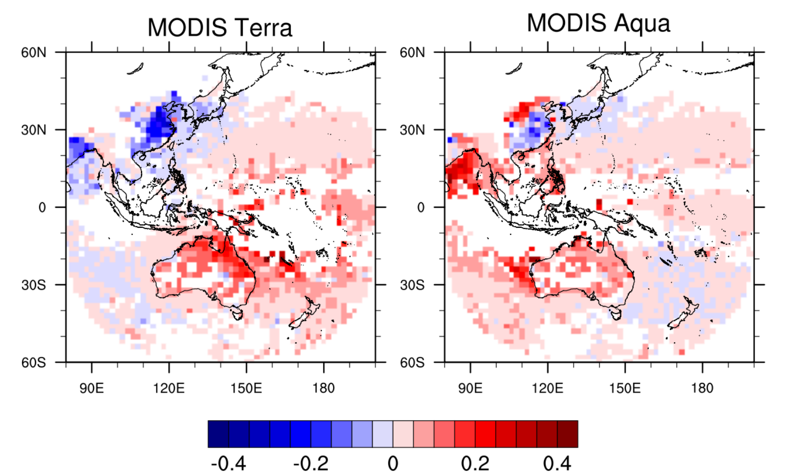

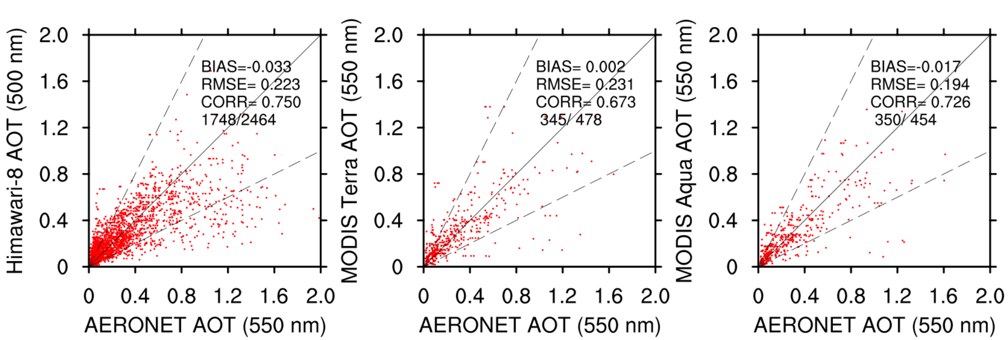

The observation frequencies of Himawari-8 are generally much **higher** than that of MODIS, especially over the **NCP, India, and Australia areas**, and they are generally **comparable to** that of the ground-based AERONET.

The correlation coefficient of AERONET with Himawari-8 is **0.750**, higher than that with MODIS.

Himawari-8 can provide the data with more higher spatio-temporal observation frequencies and higher qualities than MODIS and AERONET.

Hourly observations and NICAM-Chem output (3D-LETKF .vs. 4D-LETKF)

1. Avoid frequent switching between the assimilation and model ensemble.
2. More observations are obtained to constrain the model states at each time slot due to assimilated asynchronous observations.

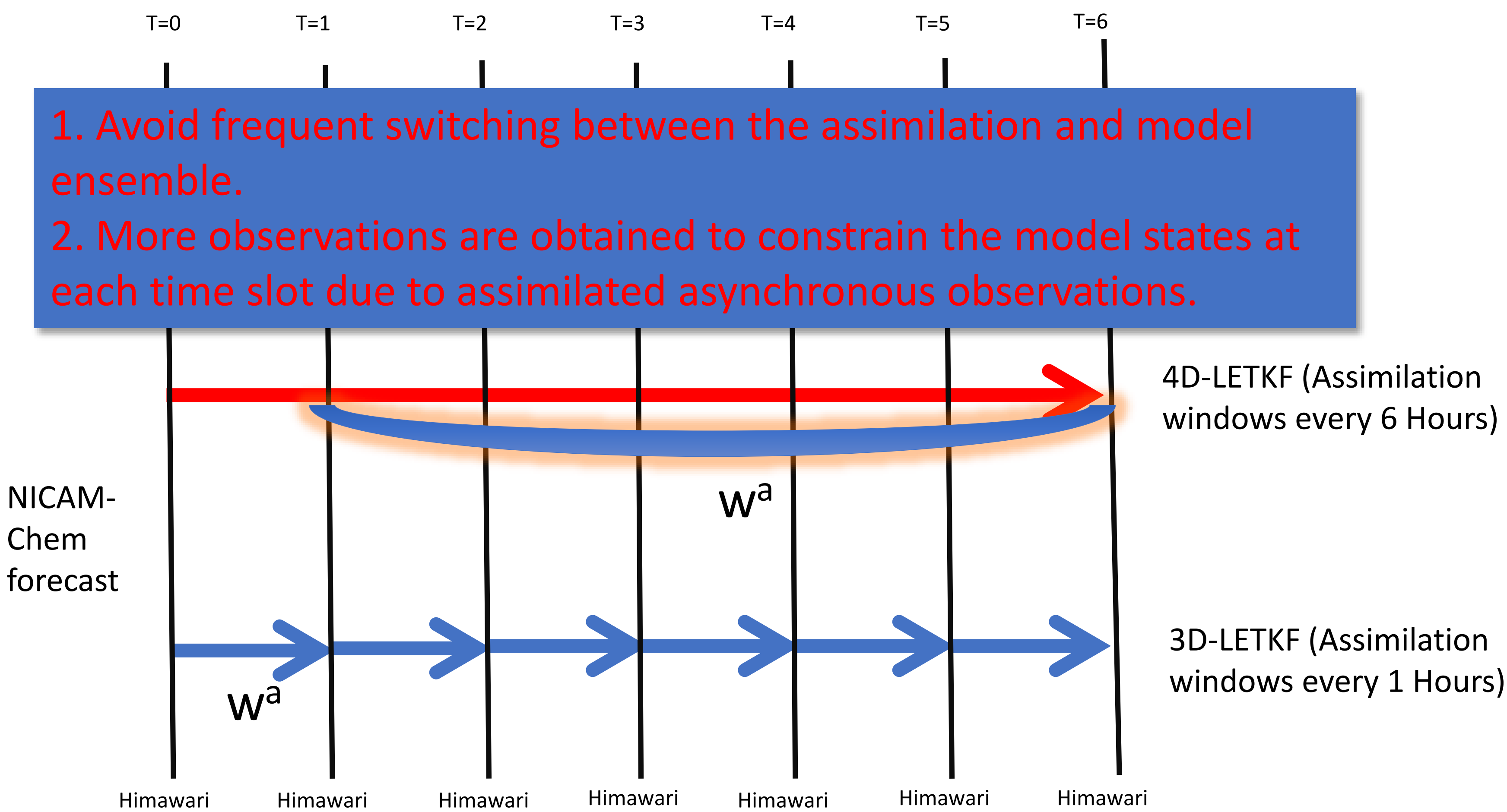

Experimental Design

Period: 2016.Nov 1 - 2016.Nov 30
Region: 60°S-60°N, 80°E-200°E

Experiment	Ensemble Number	Assimilation Window
CONTROL	1	No
LETKF	20	1 hour
4D-LETKF-6H	20	6 hour
4D-LETKF-24H	20	24 hour

Elapsed time and Observation constraint

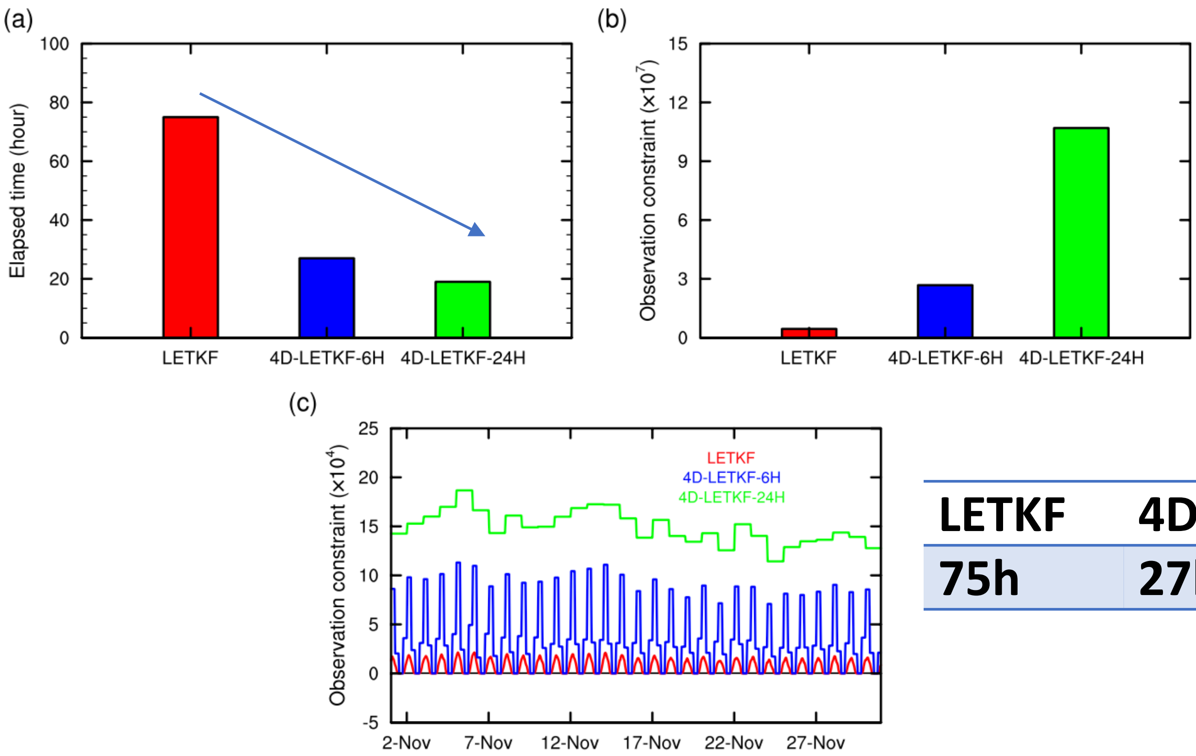

LETKF	4D-LETKF-6H	4D-LETKF-24H
75h	27h	19h

The assimilated observations for 4D-LETKF generally respond linearly to the assimilation window interval.

Most of the elapsed time of LETKF is used to set up the model frame for ensemble forecasts and assimilation.

4D-LETKF-24H can significantly enhance the computational efficiency and maximally use the daily cycle of Himawari-8-retrieved AOTs.

Comparison of the analysis with Himawari-8

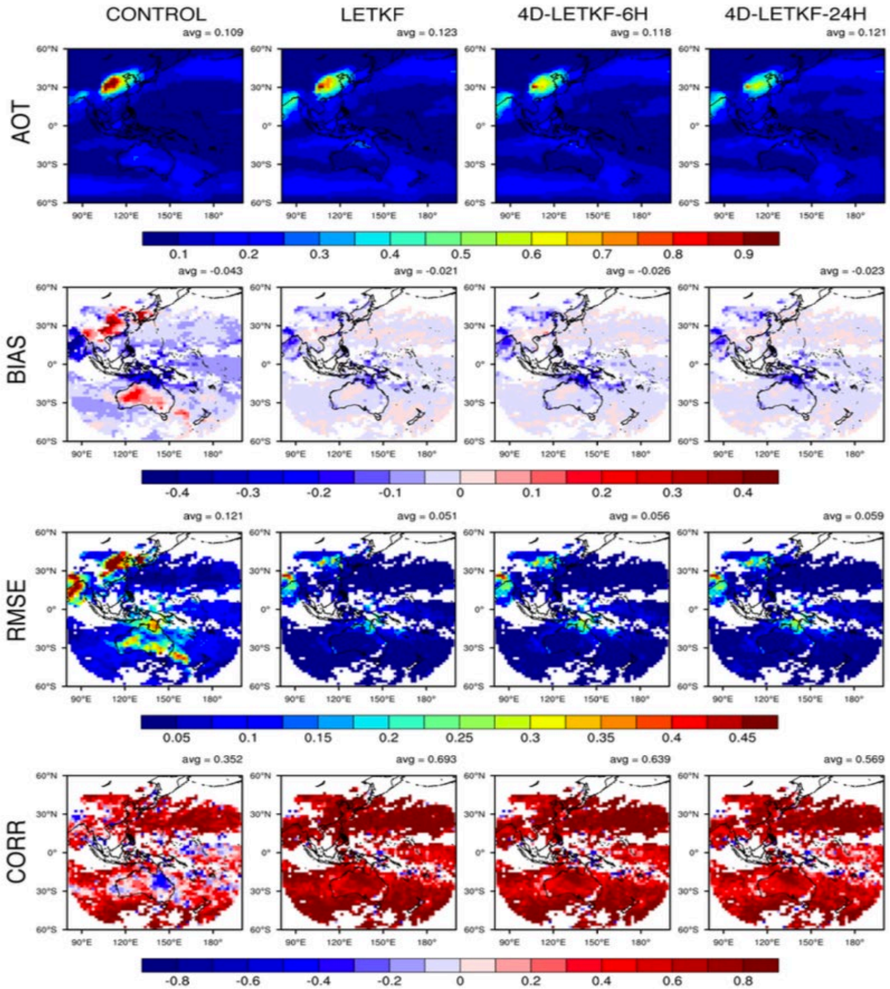

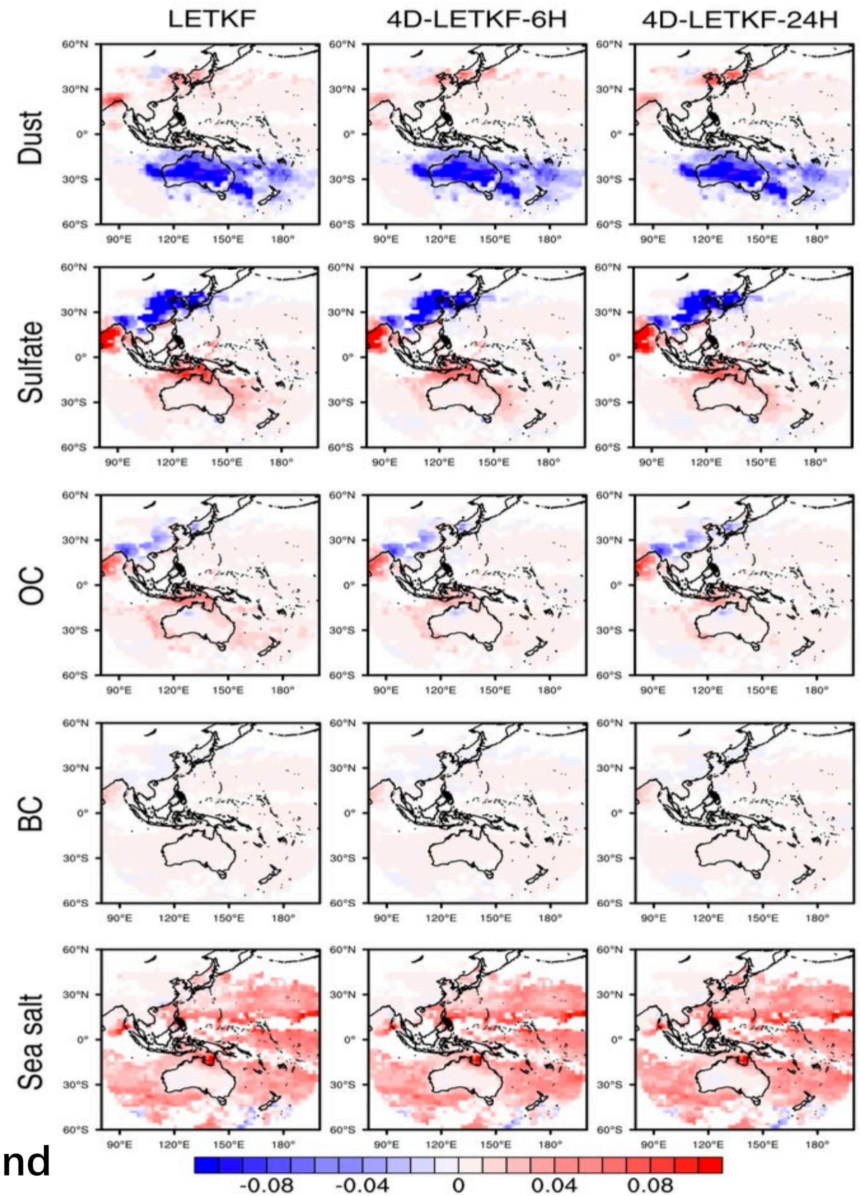

Assimilations clearly reduce the overestimation of sulfate aerosols over East Asia and dust aerosols over Australia.

The general underestimations of AOT over India and ocean areas are also corrected.

Comparison of the analysis with Himawari-8

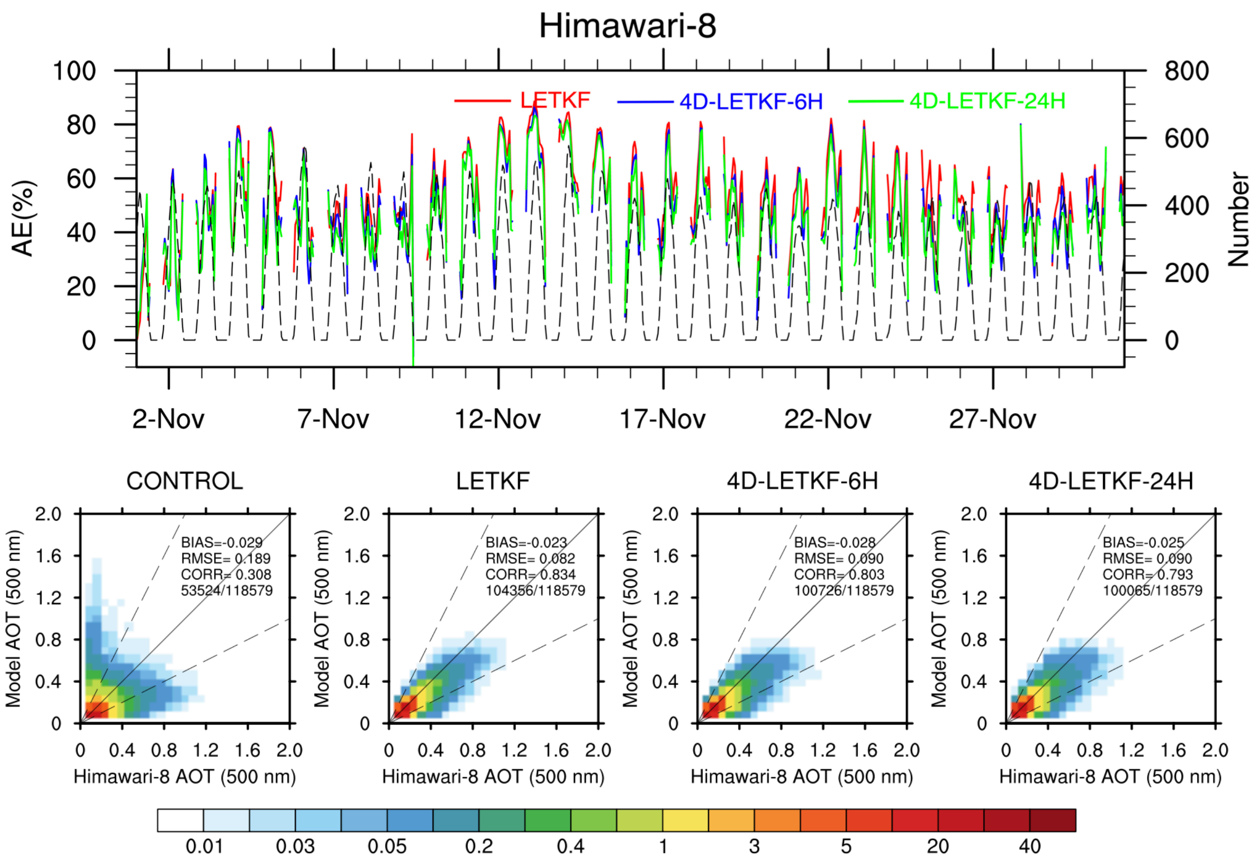

$$AE = \frac{rmsd_f - rmsd_a}{rmsd_f} \times 100\%$$

(Yumimoto et al., 2016)

The AEs are mostly positive, indicating that assimilations positively affect the model performances.

The correlation coefficients of assimilation results with Himawari-8 are all higher than 0.79.

Comparison of the analysis with AERONET

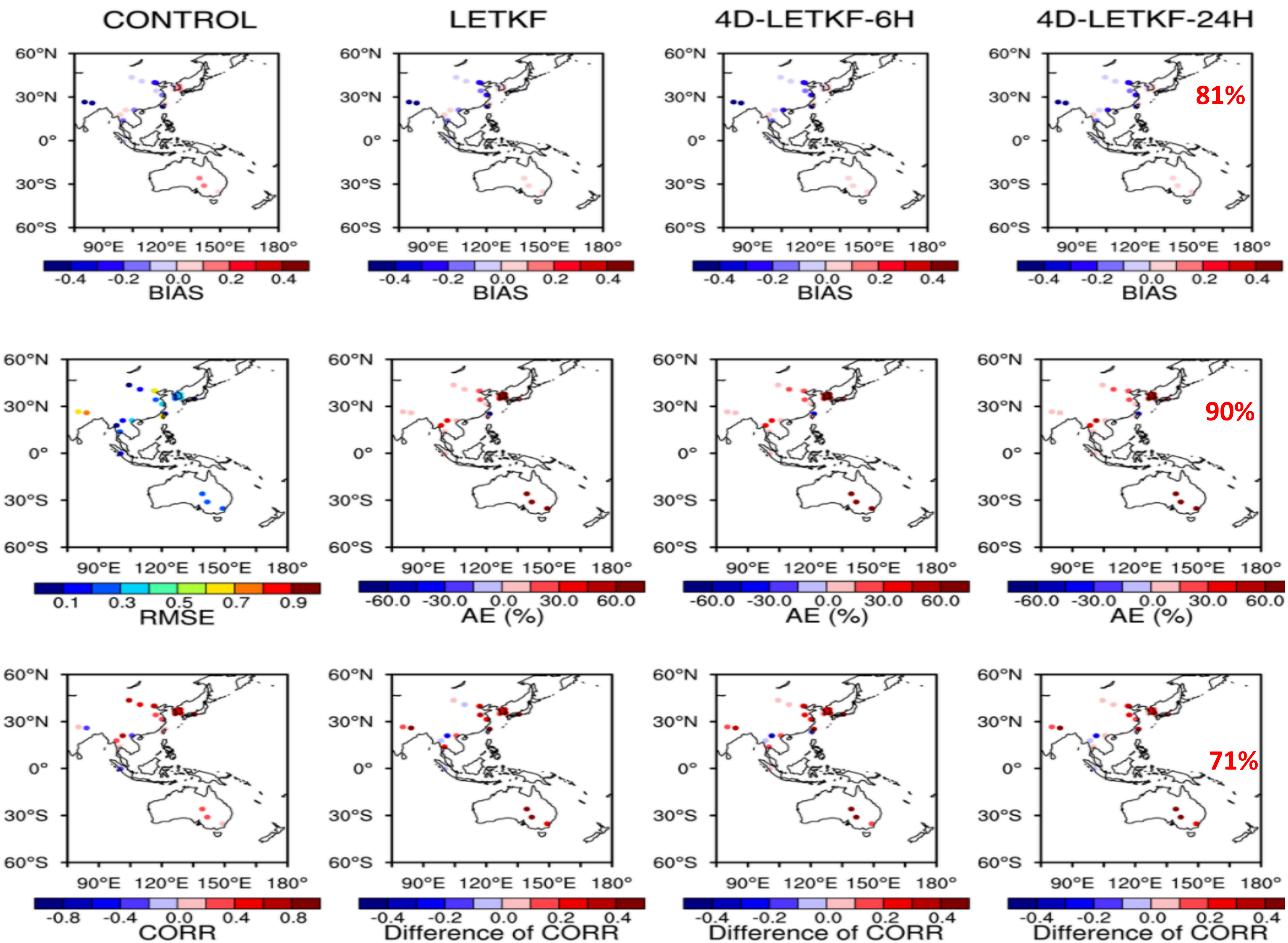

Evaluation of the temporal evolutions of AOTs with the AERONET

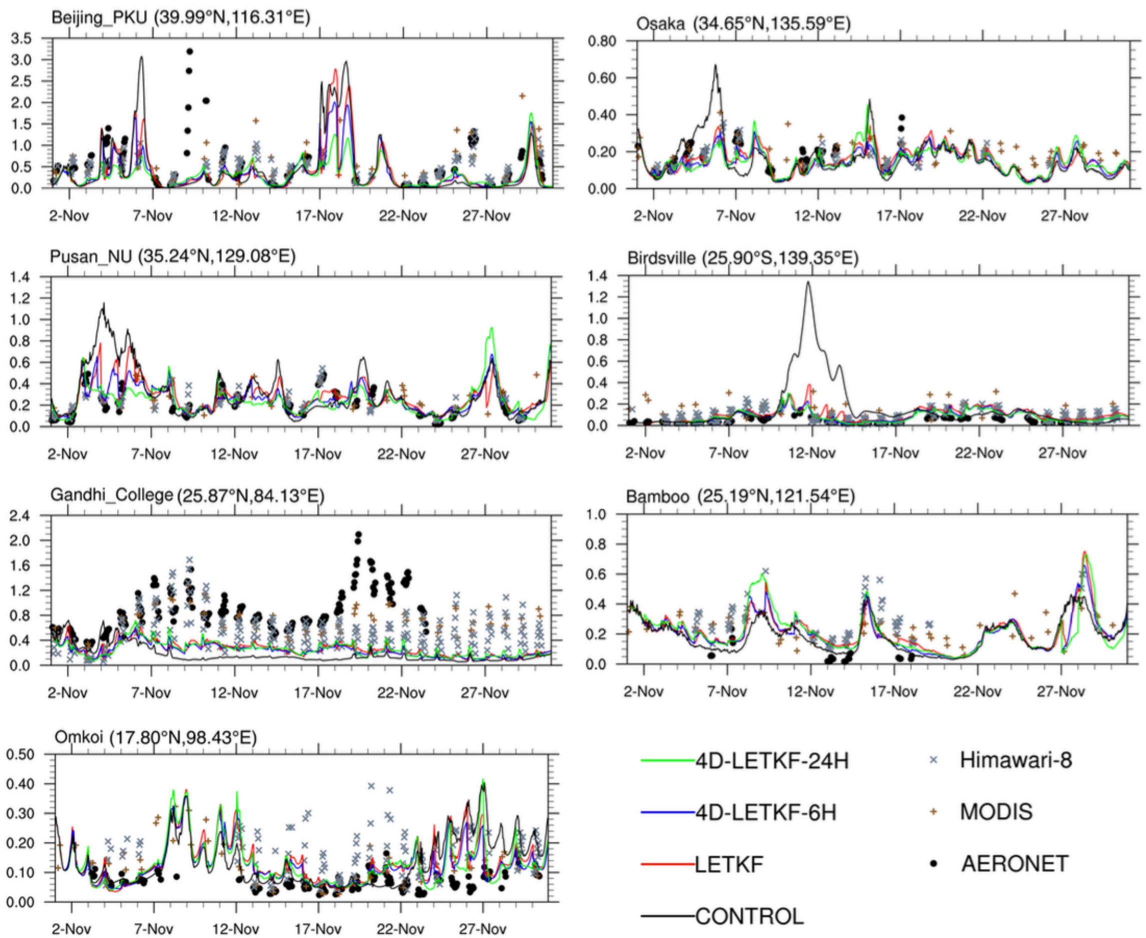

Assimilation can better reproduce the temporal variations of aerosols.

It is difficult to improve the obviously underestimated sites.

There are some differences between satellite-retrieved data and AERONET ones.

Comparison of the analysis with MODIS

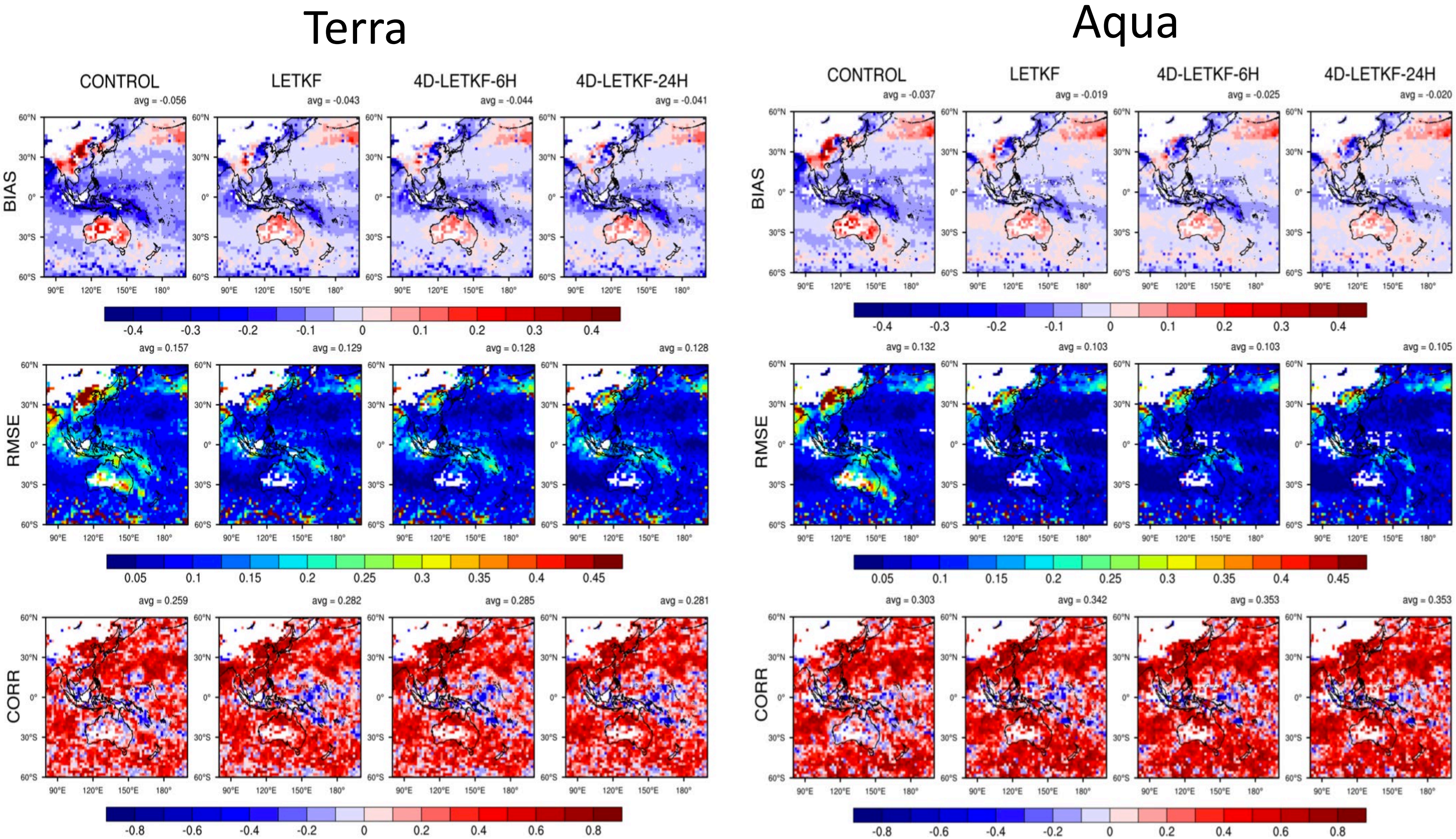

The analyses can also better reproduce the spatial and temporal variations of the MODIS AOT observations.

4D-LETKF NICAM-Chem 72 hours forecast system

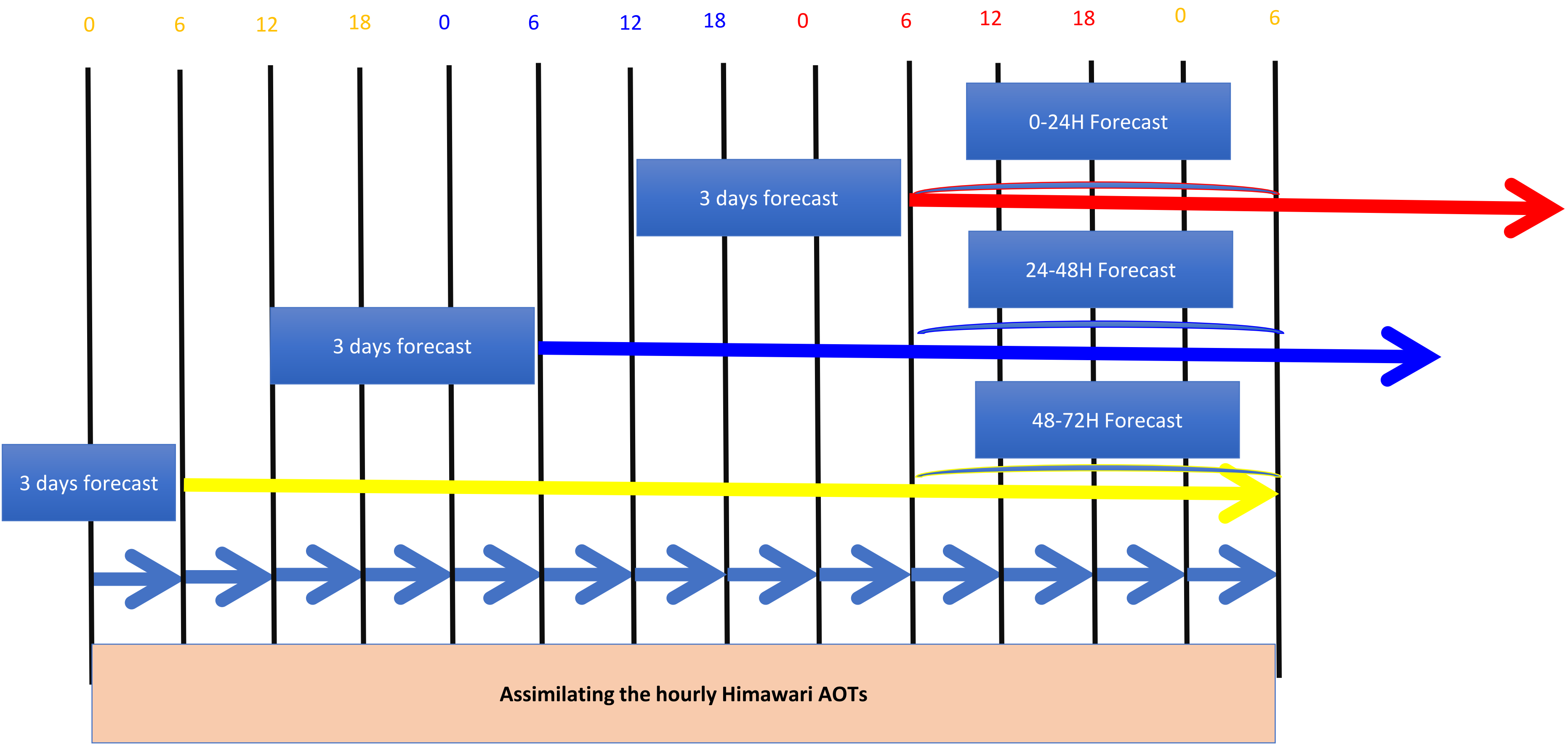

Evaluation of the 72h AOD forecast with assimilation of Himawari-8

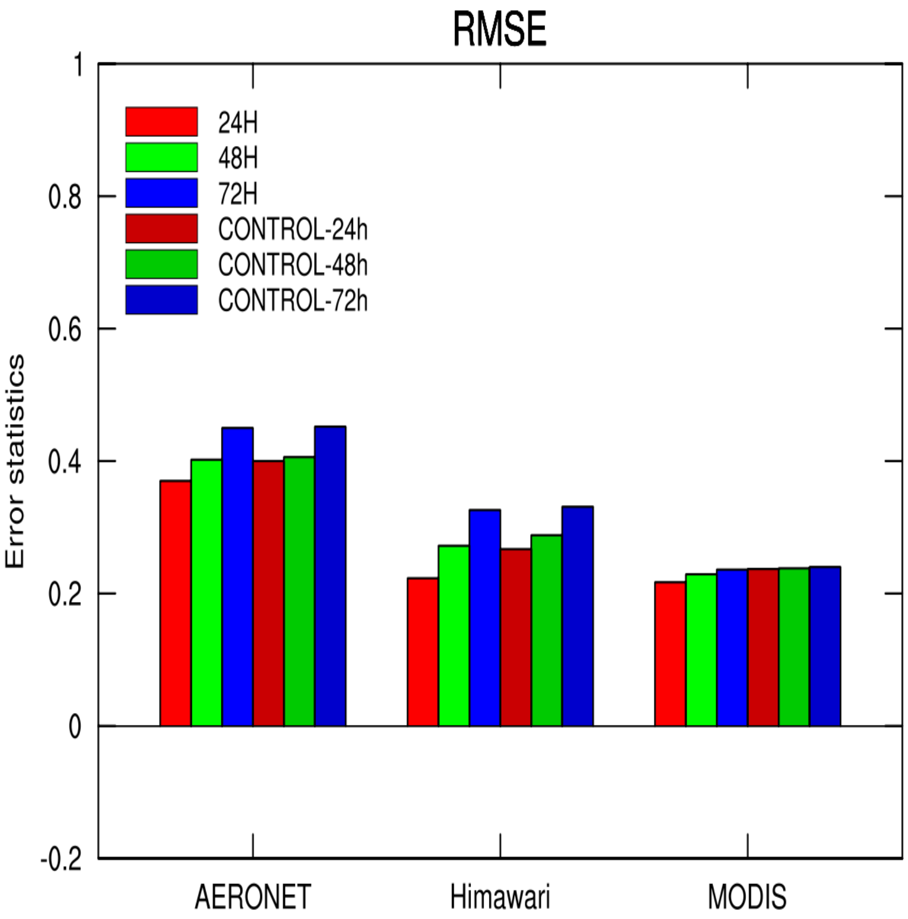

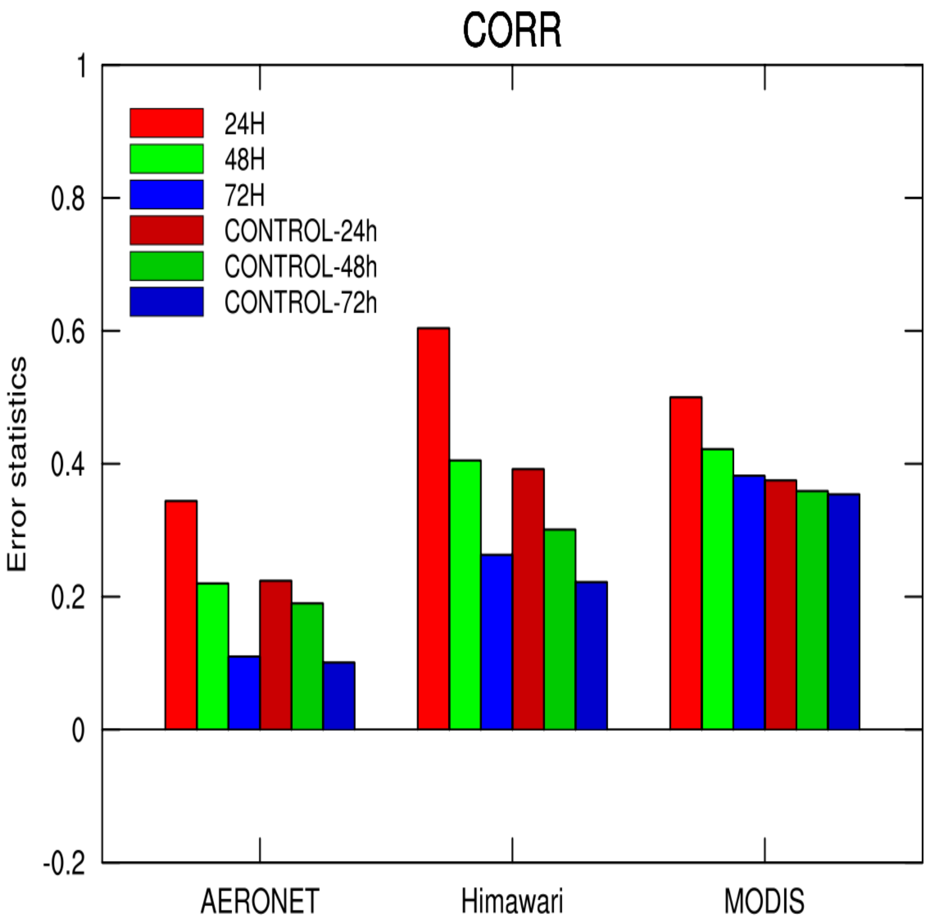

In the first 24 hours, whether improving the initial condition has obvious effects on the results.

After 48 hours, the effects of initial condition on the forecast results are very weak.

Evaluation of the 72h forecast $PM_{2.5}$ concentration (RMSE)

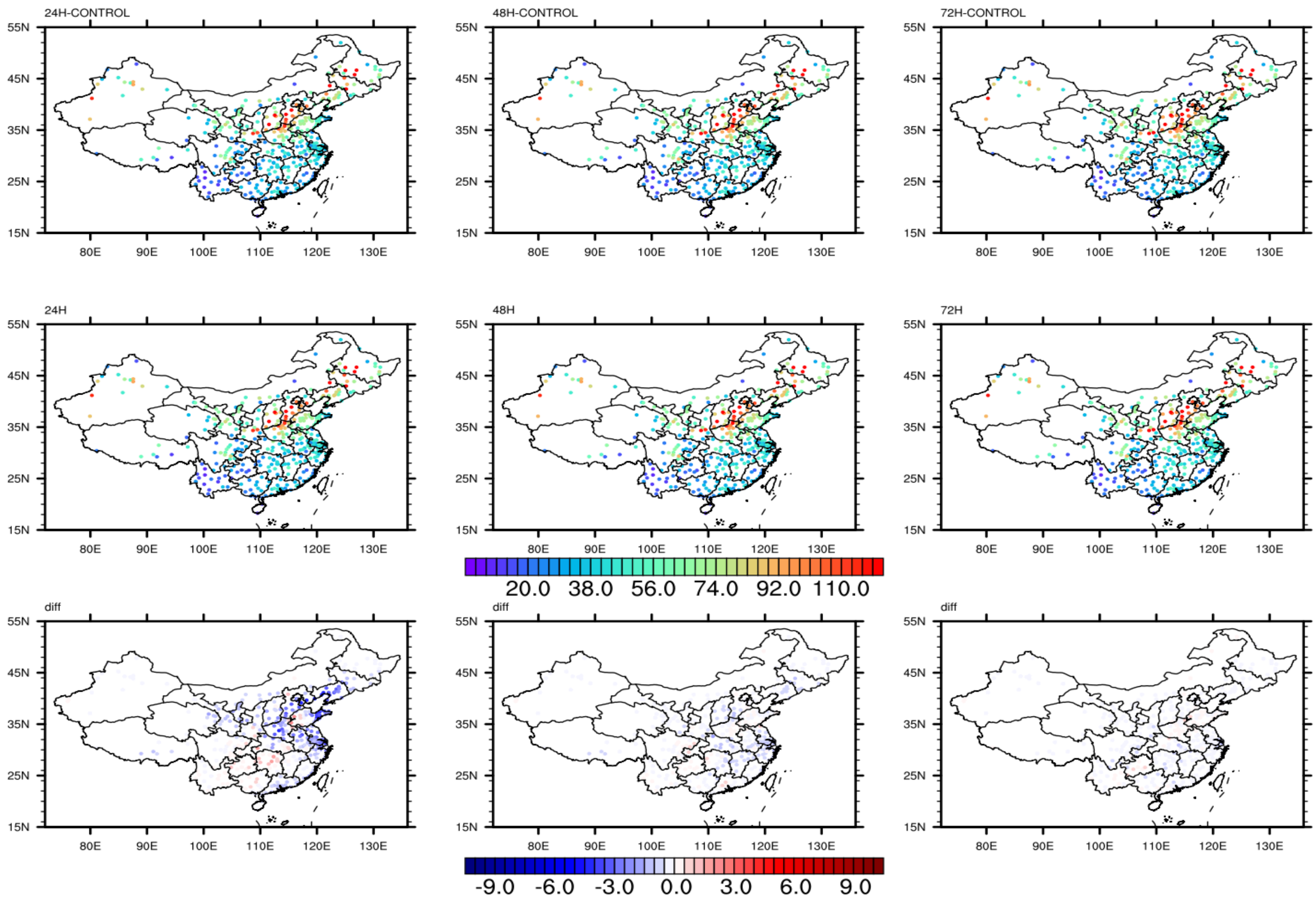

Experiment	24H	48H	72H
RMSE	292(80%)	299(82%)	302(83%)

Evaluation of the 72h forecast PM_{10} concentration (RMSE)

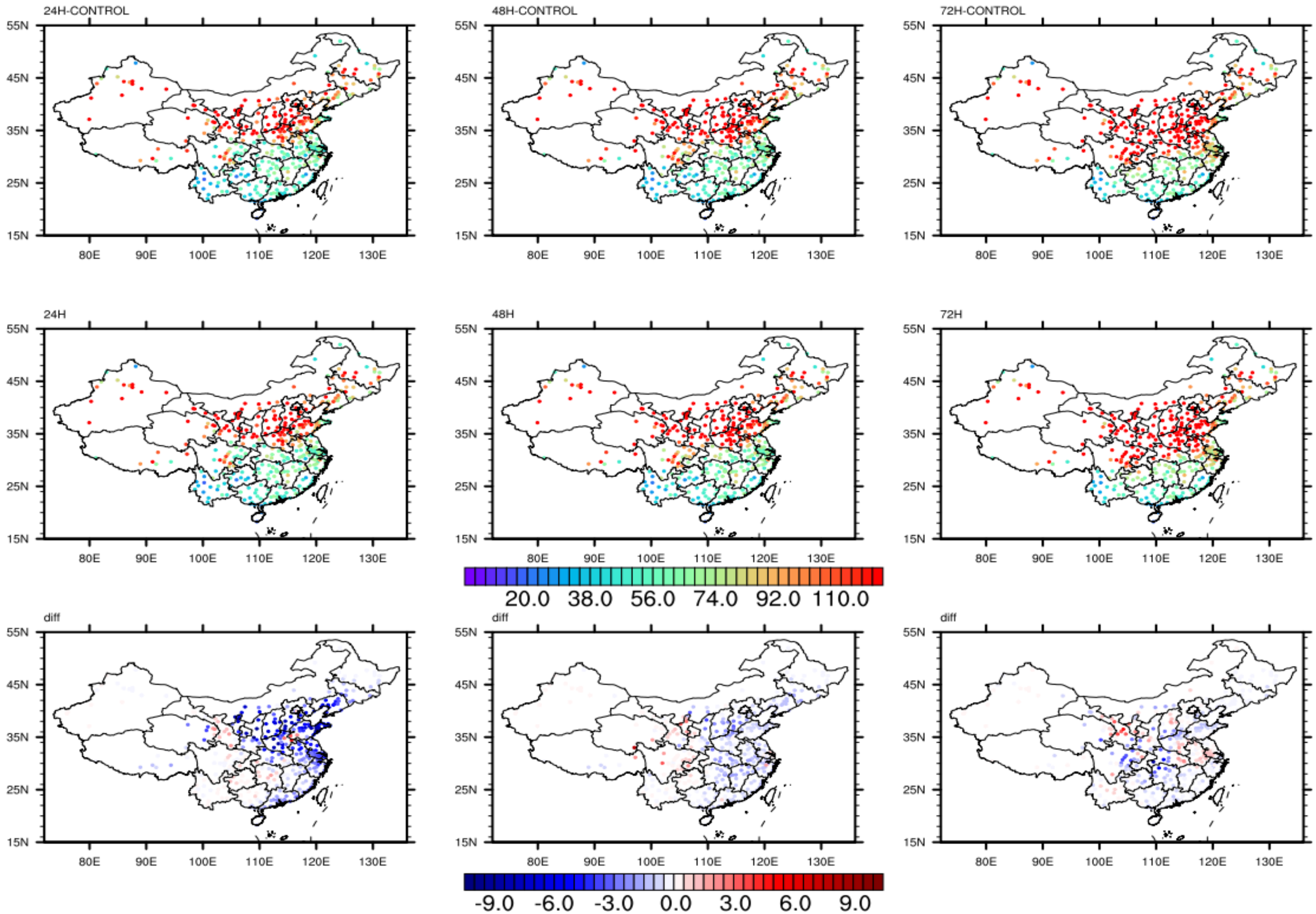

Experiment	24H	48H	72H
RMSE	298(82%)	281(77%)	251(69%)

Aerosol vertical data assimilation using CALIPSO (preliminary results)

RMSE between CONTROL experiment and CALIPSO

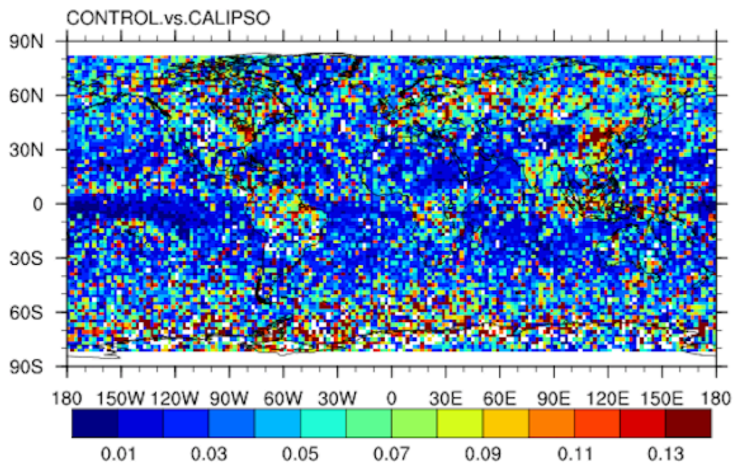

RMSE between Assimilation experiment and CALIPSO

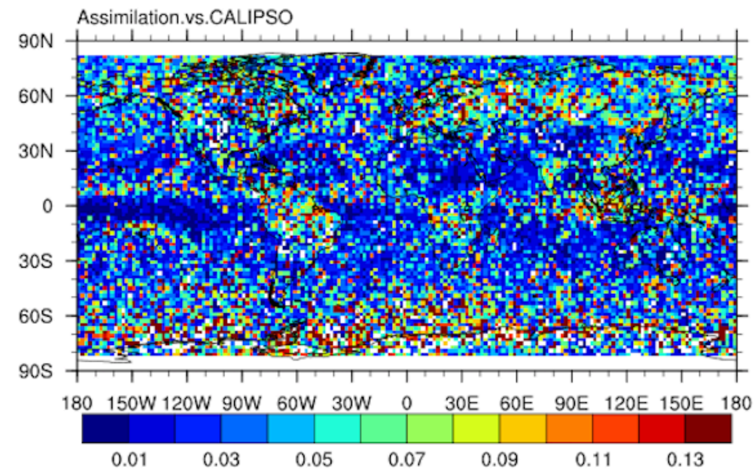

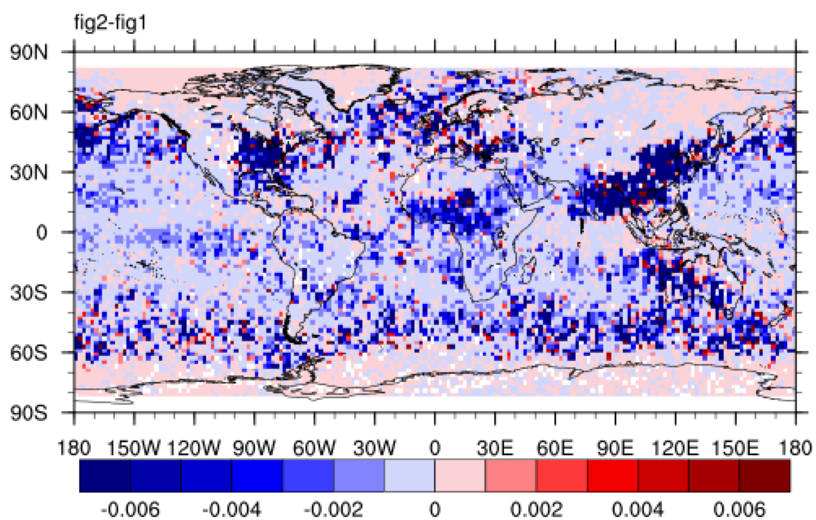

The difference between the RMSE of CONTROL and RMSE of CAIPSO shows the obvious decreasing of RMSE in many parts especially in Asia.

Summary

1. We successfully develop a LETKF and 4D-LETKF aerosol assimilation system for NICAM, which are applied to assimilate both the polar and geostationary satellite observations such as the MODIS and Himawari-8.
2. One month hourly aerosol analyses are generated with the 4D-LETKF system, which can significantly improve the calculation efficiency. The aerosol analyses are more comparable to both the assimilated Himawari-8 AOTs and independent AERONET and MODIS AOTs. The assimilation system correctly reduce the overestimation of the AOTs over East China, which are probably due to the reduction of emissions in China recently.
3. The assimilation of Himawari-8 AOTs can also correct the aerosol initial conditions and emissions, improving the aerosol forecast especially over the first 24 hours.

Thank you！